

Self-interaction correction with Wannier functions

Massimiliano Stengel¹ and Nicola A. Spaldin¹

¹*Materials Department, University of California, Santa Barbara, CA 93106-5050, USA*

(Dated: November 15, 2018)

We describe the behavior of the Perdew-Zunger self-interaction-corrected local density approximation (SIC-LDA) functional when implemented in a plane-wave pseudopotential formalism with Wannier functions. Prototypical semiconductors and wide-bandgap oxides show a large overcorrection of the LDA bandgap. Application to transition-metal oxides and elements with d electrons is hindered by a serious breaking of the spherical symmetry, which appears even in a closed shell free atom. Our results indicate that, when all spherical approximations are lifted, the general applicability of orbital-dependent potentials is very limited and should be reconsidered in favor of rotationally invariant functionals.

PACS numbers: 71.15.-m

I. INTRODUCTION

Within the Kohn-Sham approach to density functional theory, the total energy of a many-electron system of density $\rho = \rho_{\uparrow} + \rho_{\downarrow}$ is generally decomposed into four terms:

$$E^{KS} = T_s + E_H[\rho] + E_{ext} + E_{xc}[\rho_{\uparrow}, \rho_{\downarrow}]. \quad (1)$$

These terms describe the kinetic energy of the fictitious set of one-particle orbitals T_s , the Hartree energy E_H , the energy due to the interaction with the external potential E_{ext} , and the unknown exchange and correlation energy E_{xc} ; the latter is commonly approximated by local or semi-local functionals of the density such as the local density (LDA) or generalized gradient (GGA) approximations.

Despite the innumerable successes of the LDA and GGA, some serious drawbacks exist that prevent the applicability of these methods to a wider range of materials and phenomena. Situations in which these standard functionals lead to qualitatively incorrect physics include the erroneous prediction of metallicity for magnetic transition metal oxides, an inability to localize defect states in solids¹ and unpaired electrons in water², qualitatively incorrect metallic transport for single-molecule junctions³, inaccurate redox potentials and charge-transfer reactions⁴, and unphysical fractionally charged fragments in the molecular dissociation limit⁵. These failures can be traced, at least in part, to the self-interaction error (SIE), which is the spurious interaction of an electron with its own Hartree and exchange-correlation potential. Indeed, in the case of one-electron systems such as the ground state of the hydrogen atom, E_H and E_{xc} should cancel exactly:

$$E_H[\rho_{1s}] + E_{xc}[\rho_{1s}, 0] \quad \text{should equal} \quad 0,$$

but this condition is not fulfilled by approximate exchange-correlation functionals such as LDA or GGA. While in a many-electron system the notion of self-interaction is less clear cut, it is commonly accepted that

this same mechanism affects the behavior of strongly localized, atomic-like orbitals, such as d states in transition metal compounds, by suppressing or mistreating on-site Coulomb interactions. The considerable fundamental and technological interest in d -electron systems such as high- T_c superconductors and colossal magnetoresistive manganites provides a compelling incentive for implementing appropriate SIE-free density functional methods. Interestingly, the SIE has a relatively minor impact on total energies, but it strongly affects the eigenvalues of the Kohn-Sham Hamiltonian. In particular, the energy eigenvalue associated with the highest occupied orbital usually shows a strong departure from the ionization potential, while it should match it exactly within exact DFT⁶.

Attempts to correct the self interaction error can be traced back to the seminal paper by Perdew and Zunger (PZ)⁷, who defined the self-interaction corrected (SIC) exchange-correlation energy, E_{xc}^{SIC} , as

$$E_{xc}^{SIC} = E_{xc}^{\text{approx}}[\rho_{\uparrow}, \rho_{\downarrow}] - \sum_{\alpha\sigma} (E_H[\rho_{\alpha\sigma}] + E_{xc}^{\text{approx}}[\rho_{\alpha\sigma}, 0]). \quad (2)$$

Here $E_{xc}^{\text{approx}}[\rho_{\uparrow}, \rho_{\downarrow}]$ is the approximate (for example LDA or GGA) exchange-correlation energy, and the term within the summation is the self-interaction energy of an electron in orbital α with spin σ ; $E_H[\rho_{\alpha\sigma}]$ is the self-Coulomb part and $E_{xc}^{\text{approx}}[\rho_{\alpha\sigma}, 0]$ is the self exchange-correlation part. For isolated atoms, this approach yielded Hamiltonian eigenvalues which were in surprisingly good agreement with experimental removal energies.

These successes motivated a considerable subsequent effort to incorporate PZ self-interaction corrections in calculations for solids. Unfortunately, however, direct implementation of the PZ functional in extended systems has proved to be technically non-trivial. The main issue arises from the fact that the SIC-LDA functional, unlike standard Kohn-Sham theories, is not invariant with respect to a unitary transformation of the occupied manifold; in particular, the SIC vanishes for extended Bloch wavefunctions. Therefore, the first challenge of any im-

plementation is to devise a general and physically sound criterion for the choice of this unitary transformation, which yields a set of “local orbitals” (LO), as opposed to the “canonical orbitals” (CO) which are the usual eigenstates of the Hamiltonian with Bloch periodicity.

Soon after the initial work by Perdew and Zunger, Heaton Harrison and Lin (HHL) recognized that Wannier functions provide an ideal basis for describing the localized-delocalized duality of electrons in the full-SIC Hamiltonian⁸; by implementing SIC-LDA within a LCAO basis set HHL found considerable improvement in the solid Ar and LiCl bandstructures. An appealing aspect of the HHL approach is the introduction of a unified Hamiltonian by means of band projections. This strategy removes the orbital dependence of the SIC Hamiltonian and allows for the calculation of all SIC-LDA eigenvalues for a given k point by one single matrix diagonalization. Furthermore, HHL defined the unitary transformation between the Wannier and Bloch representation as the one yielding the variational minimum of the SIC-LDA functional within the usual orbital orthonormality constraints. Pederson, Heaton and Lin⁹ later demonstrated that the so-called “localization condition” is then fulfilled by the localized orbitals ϕ_α and their associated SIC potentials δV_α :

$$\langle \phi_\alpha | \delta V_\alpha - \delta V_\beta | \phi_\beta \rangle. \quad (3)$$

This means that the Lagrange multiplier matrix enforcing the orthonormality condition is Hermitian, and it can be indeed diagonalized to obtain the SIC eigenvalue spectrum, together with a set of eigenvectors that correspond to the Bloch-periodic COs.

Svane and Gunnarsson¹⁰ (SG) and later Szotek, Temmerman and Winter¹¹ (STW) applied a fully self-consistent SIC-LDA method to extended systems within an LMTO-ASA (linear muffin tin orbital - atomic sphere approximation) implementation, obtaining remarkable results for both d - and f -electron materials. A major pitfall of the SIC functional is that it allows for multiple local minima, one of these being the trivial solution where all the LOs are Bloch-like (i.e. no SIC is applied), and another obvious one being the one where all the LOs are Wannier-like; intermediate (mixed) choices also exist, where some of the LOs are Wannier-like, and others keep their itinerant character. SG and STW proposed choosing the solution with the lowest total energy (which corresponds to the absolute minimum of the SIC functional, and is consistent with the variational character of the localization procedure). Based on this choice, phase transitions are sometimes observed as a function of external parameters (e.g. volume) in which the SIC contribution for a given band becomes positive (or negative); this crossover between SIC and no SIC is rationalized in terms of a physically appealing realization of Mott transitions (which are driven by the competition between bandwidth and on-site Coulomb repulsion).

Some fundamental problems with the use of a partially Bloch-like and localized solution have been pointed out,

however, by Arai and Fujiwara¹² (AF). First, the presence of “delocalized” bands to which no SIC is applied leads to a severe size-consistency problem when the extended solid is considered as the thermodynamic limit of an increasingly large cluster where SIC is unavoidably finite¹². Even in regions where the SIC energies are slightly positive the SIC potentials remain strongly attractive, so when the cluster volume is increased to the thermodynamic limit strong and unphysical changes in the eigenvalue spectrum must be expected. Second, the sign of the SIC energy (and hence whether or not the orbitals are treated as localized) is sensitive to details such as the parameterization of the LSDA. Since the main aim of the SIC method is to correct for the self-exchange error, qualitative differences in the electronic ground state determined solely by minor details of the correlation functional are, again, physically hard to justify.

Interestingly, AF also discussed the consequences of the sphericalization of the SIC potential, which is routinely performed (see SG and STW) within LMTO implementations and was also adopted in the early works of HHL⁸. While a significant impact on the bandstructure of solids and unphysical energy splittings within otherwise crystal-symmetric multiplets were found, AF concluded that the overall consequences of this approximation were relatively unimportant.

It has been shown recently for a wide range of atoms that orbitals with different angular momenta are allowed to mix upon lifting the spherical approximation¹³. For example $3s$ and $3p$ states in Ar mix to yield four tetrahedrally symmetrical sp^3 hybrids, analogous to the maximally localized Wannier functions in sp compounds¹⁴. As a consequence of this mixing, the SIC energy becomes *negative* for all bands, while it is generally positive for pure p states; furthermore, eigenvalue shifts of the order of 1 eV occur, and in general the agreement with experiments tends to worsen¹³. These atomic results suggest that, while the sphericalization of the SIC potential itself has a very minor *direct* impact, in agreement with the conclusions of Refs. 8 and 12, it might well have a dramatic *indirect* impact, by preventing the true variational minimum of the SIC functional from being found. In particular, if the total energy criterion for the selection of the localized/delocalized bands is enforced, the artificial suppression of interband mixing might lead to erroneous choices, and qualitatively incorrect electronic ground states; for example, oxygen $2p$ states, that are considered to be itinerant within the spherical approximation^{10,11} can become localized once mixing with oxygen $2s$ states is allowed.

It is apparent from the above analysis that two main issues affect self-interaction corrected calculations for extended solids, i) the existence of multiple local minima and ii) the validity of the spherical approximation. In this work we address both issues by using modern Wannier-function theory¹⁵ and a plane-wave norm-conserving pseudopotential formalism. By testing our

method on simple atomic systems we first demonstrate that, if used with care, the pseudopotential approximation introduces a negligible error with respect to the most accurate all-electron results available to date¹³; this provides a strong validation of our results and contributes to putting the full-SIC formalism onto a solid implementation-independent technical footing. In particular, in agreement with Ref. 13, we find that the spherical approximation has an important impact on the eigenvalue spectrum of solids, often significantly worsening the agreement with experimental spectroscopic data. We further find that, within our spherically-unrestricted SIC-LDA, the fully localized solution is always the variational electronic ground state, even in bulk Si where the valence electrons are usually considered as being itinerant; this result suggests that some caution must be taken when interpreting the localized/delocalized SIC crossover in terms of a Mott transition, since it might be an artifact of the numerical approximations used. Finally, in our implementation two further pitfalls of the SIC-LDA method emerge, which were so far overlooked in the literature: i) the giant overcorrection of the electronic band gaps in solids and ii) the unphysical breakdown of crystal point symmetry, which is especially serious in d -electron systems. We rationalize these effects in terms of, respectively, lack of proper treatment of dielectric screening and the rotational non-invariance of the method. Our results provide useful guidelines for further research in the quest for an improved density functional, and also a benchmark against which approximate flavors of SIC^{16,17,18} can be tested and validated.

The remainder of this work is organized as follows. In Sec. II we give a detailed overview of the SIC technique we use in this work. In Sec. III we present our results: First we validate our method by performing some tests on simple atomic systems, then we apply SIC to simple, prototypical solids (Ar, Si, MgO) and finally, we analyze the performance of SIC for d -electron systems. In Sec. IV we discuss these results in light of previously reported studies and analyze their impact for future methodological development. In Sec. V we summarize and conclude. The Appendix presents an analysis of Boys orbitals in d -electron spherically symmetric atoms; this analysis extends the work by Posternak¹⁴ for sp elements, and shows that orbital-dependent functionals tend to unphysically break the symmetry of closed-shell atoms.

II. METHOD

Before presenting our method we briefly summarize some basic notations and conventions that will be useful in the derivation (for a more extensive treatment see Ref. 19 and references therein). We assume a Born-von Kármán supercell of volume $\Omega_{BvK} = N\Omega$, where N is the total number of k points arranged on a regular three-dimensional mesh and Ω is the volume of the primitive cell used to represent the periodic crystal. The gener-

alized Bloch orbitals $\psi_{n\mathbf{k}}(\mathbf{r})$ (which are not necessarily eigenstates of the Hamiltonian) can be written in terms of the cell-periodic functions $u_{n\mathbf{k}}(\mathbf{r})$:

$$\psi_{n\mathbf{k}}(\mathbf{r}) = e^{i\mathbf{k}\cdot\mathbf{r}} u_{n\mathbf{k}}(\mathbf{r}) \quad ;$$

the latter can be represented in reciprocal space as follows:

$$\tilde{u}_{n\mathbf{k}}(\mathbf{G}) = \frac{1}{\sqrt{\Omega}} \int_{\text{cell}} e^{-i\mathbf{G}\cdot\mathbf{r}} u_{n\mathbf{k}}(\mathbf{r}) d\mathbf{r} \quad .$$

The reciprocal lattice vectors \mathbf{b} of the Born-von Kármán supercell can be written in terms of \mathbf{G} and the k -point mesh:

$$\mathbf{b} = \mathbf{G} + \mathbf{k} \quad ,$$

and the Wannier function associated with the band n and the lattice site \mathbf{R} in reciprocal space is:

$$\tilde{w}_{\mathbf{R}n}(\mathbf{b}) = \frac{1}{\sqrt{N}} e^{-i\mathbf{b}\cdot\mathbf{R}} \tilde{u}_{n\mathbf{k}}(\mathbf{G}) \quad . \quad (4)$$

We will set $\mathbf{R} = 0$ in the remainder of the paper, and thus focus on the minimal set of Wannier functions which is necessary to describe the solid; also we will introduce a spin index σ . Upon Fourier transformation one obtains the Wannier functions $w_{n\sigma}(\mathbf{r})$ in real space and their associated charge density distributions $\rho_{n\sigma}(\mathbf{r}) = |w_{n\sigma}(\mathbf{r})|^2$. The self-interaction energy of the system, which needs to be added to the LDA (or GGA) total energy, is then given by Eqn. 2.

In order to minimize the SIC-LDA functional we need to calculate gradients of the SIC energy with respect to the wavefunction plane-wave coefficients. We start by calculating the gradients of the SIC energy with respect to the Wannier functions, which can be written as:

$$\frac{\delta E^{SIC}}{\delta w_{n\sigma}^*(\mathbf{r})} = \hat{V}_{n\sigma}^{SIC}(\mathbf{r}) w_{n\sigma}(\mathbf{r}) \quad .$$

Here $\hat{V}_{n\sigma}^{SIC}$ is the SIC (Hartree plus exchange and correlation) potential generated by the Wannier density $\rho_{n\sigma}(\mathbf{r})$. The state-dependent potential $\hat{V}_{n\sigma}^{SIC}$ can be recast into a unified operator by using band projections:

$$\hat{V}^{SIC} = \sum_{n\sigma} \hat{V}_{n\sigma}^{SIC} |w_{n\sigma}\rangle \langle w_{n\sigma}| \quad . \quad (5)$$

In general, \hat{V}^{SIC} has nonzero Hermitian and anti-Hermitian components:

$$\hat{V}^{SIC-H} = \frac{1}{2} (\hat{V}^{SIC} + \hat{V}^{SIC\dagger}) \quad (6)$$

$$\hat{V}^{SIC-A} = \frac{1}{2} (\hat{V}^{SIC} - \hat{V}^{SIC\dagger}) \quad . \quad (7)$$

When applied to the electronic wavefunctions, the anti-Hermitian part \hat{V}^{SIC-A} produces a unitary mixing within the occupied manifold and is the signature of the

rotational non-invariance of the SIC-LDA functional; no such term exists in standard Kohn-Sham theories. The Hermitian term, on the other hand, evolves the electronic subsystem in a direction which is perpendicular to the occupied subspace, and can be treated as an additional term to be added to the Kohn-Sham Hamiltonian. For reasons of transparency and in order to have better control over the minimization process we decided to separate the two tasks into two nested loops.

In an inner loop, we constrain the update of the wavefunctions to a unitary mixing within the occupied manifold:

$$u'_{n\mathbf{k}}(\mathbf{r}) = \sum_m u_{m\mathbf{k}}(\mathbf{r}) U_{mn}^{(\mathbf{k})} \quad ,$$

and we seek the set of unitary matrices $U^{(\mathbf{k})}$ that yields the minimum value of the SIC energy (the standard Kohn-Sham energy is invariant with respect to this transformation). This operation is formally analogous¹⁹ to the calculation of the maximally localized Wannier functions for a set of entangled energy bands¹⁵, except that, instead of minimizing the quadratic spread, here we need to enforce the representation with the minimum value of the Perdew-Zunger self-interaction. In particular, the rotation matrices are obtained by adding an infinitesimal anti-Hermitian matrix to the identity:

$$U^{(\mathbf{k})} \sim 1 + dW^{(\mathbf{k})} \quad ;$$

the variation of the SIC-LDA functional with respect to this transformation is provided by \hat{V}^{SIC-A} :

$$\left(\frac{dE^{SIC}}{dW^{(\mathbf{k})}} \right)_{mn} = \langle \psi_{m\mathbf{k}} | \hat{V}^{SIC-A} | \psi_{n\mathbf{k}} \rangle \quad .$$

It is then easy to show that the stationarity of the functional (zero gradient) implies:

$$\langle w_m | V_n - V_m | w_n \rangle = 0 \quad ,$$

which is the usual ‘‘localization condition’’²⁰.

In the outer loop we add to the LDA Hamiltonian the Hermitian part of the SIC operator:

$$\hat{H}^{SIC-LDA} = \hat{H}^{LDA} + \hat{V}^{SIC-H} \quad ,$$

which is now identical to the full SIC operator since the anti-Hermitian part vanishes within the subspace spanned by the occupied bands. We then take standard electronic steps until the ground state is reached. At self-consistency, the eigenvalues of this SIC Hamiltonian formally agree with the eigenvalues of the Lagrange multiplier matrix that can be obtained within direct minimization techniques²¹.

We note that particular care must be taken in the correct evaluation of the self-Hartree energy and potential of the Wannier charges, since the periodic boundary conditions induce some spurious long-range interactions between the localized charge distributions. While some authors²² have proposed to truncate the $1/r$ Coulomb interaction to eliminate the divergence for $\mathbf{G} = 0$, in this work

we use the standard approach of introducing a uniform background charge to neutralize the system:

$$E_0^H[\rho] = \frac{1}{2} \frac{4\pi}{\Omega_{BvK}} \sum_{\mathbf{b} \neq 0} \frac{|\rho(\mathbf{b})|^2}{b^2} \quad . \quad (8)$$

For a cubic BvK cell of dimension L , the error due to the use of periodic boundary conditions can be corrected up to the order $\mathcal{O}(L^{-5})$ by the following term²³:

$$E_{corr}^H = \frac{\alpha}{2L} + \frac{2\pi}{3L^3} \int_{cell} d^3r \rho_n(\mathbf{r} - \mathbf{r}_0) r^2, \quad (9)$$

where \mathbf{r}_0 is the center of the Wannier function charge. We use the same form for the Hartree potential, which is the analytic derivative of the above term with respect to the charge density ρ_n ; the relationship $E^H = 1/2 \int V^H \rho d^3r$ is exactly respected.

For both the inner and the outer loops we use a damped-dynamics minimization algorithm. For the former, we checked the internal consistency of the implementation by taking a frictionless run; the mathematical constant of motion was conserved within machine precision. The latter procedure is the standard Car-Parrinello approach with the addition of the Hermitian SIC operator. The method was implemented in an ‘‘in-house’’ electronic structure code. For all our tests we used a cubic BvK supercell, the local density approximation and norm-conserving pseudopotentials²⁴. The atomic tests were performed by using a Γ -point only sampling of the Brillouin zone and a large supercell; the above algorithm did not require any modifications, since it was constructed to be invariant with respect to Brillouin-zone folding, and hence the Γ -point only calculations are just a special case. This flexibility provides an appealing link between isolated atoms and solids, which can be treated on the same footing with the exact same computational parameters and pseudopotentials.

III. RESULTS

A. Test: *sp* atoms, Be and Ar

In order to check the reliability of our method we first apply our SIC-LDA functional to simple isolated atoms, with only *s* and *p* valence electrons. For consistency with the bulk solids, we perform these tests with the same plane-wave electronic structure code by placing the individual atoms in a large cubic cell of dimension $a_0 = 10 \text{ \AA}$. For Be we obtain the eigenvalue $\epsilon_{2s} = -9.2 \text{ eV}$ (LDA=-5.6 eV), compared to -9.1 eV recently obtained with an all-electron SIC-LDA formalism¹³. For Ar we find the same level of agreement with the all-electron SIC-LDA result¹³: $\epsilon_{3p} = -16.8 \text{ eV}$ in our calculation (LDA=-10.4 eV), compared to -16.7 eV (all-electron). It is reassuring to see that the pseudopotential frozen-core approximation, together with the adoption of periodic-boundary

conditions, has negligible influence on the accuracy of SIC-LDA in atoms, with an error of about 0.1 eV in a contribution that amounts to 3-6 eV. This favorable agreement between two very different electronic structure methods stems from the fact that the formalism (global minimum of the SIC-LDA functional with orthogonality constraints and no spherical averaging) is the same.

We note that, while the Be example is trivial (there is only one spherically symmetric s orbital, and no optimization of the “rotational” internal degrees of freedom is necessary), the Ar case has a more interesting solution in that the localized orbitals, just like the Boys orbitals, are four sp^3 hybrids with tetrahedral symmetry. The mixing of s and p orbitals is only allowed when the spherical approximation is lifted, and has dramatic consequences on orbital eigenvalues¹³. Indeed, if we artificially suppress this mixing, we obtain $\epsilon_{3p} = -15.6$ eV, a value which is quite close to the original Perdew-Zunger work ($\epsilon_{3p} = -15.8$ eV) and to the experimental ionization energy $IE=15.8$ eV. Even if the use of the spherical approximation tends to bring atomic eigenvalues in much better agreement with the experimental spectroscopic data, this procedure is ill-defined for solids and molecules and therefore cannot be used as an ingredient for a general electronic structure method; for this reason we caution against its use, as did the authors of Ref. 13.

We also note that, by suppressing the $s - p$ intermixing, the SIC energy associated with each local orbital changes radically. The four symmetric sp^3 hybrids contribute $\delta_{sp^3} = -0.45$ eV per electron, while in the restricted solution the s orbital contributes $\delta_s = -0.52$ eV and the p orbital $\delta_p = 0.15$ eV. In addition to a much higher total energy, the sphericalized solution is characterized by a positive value for δ_p . Thus, the p states might be incorrectly discarded in the variational optimization procedure once the atom is embedded in a periodic lattice¹⁰, when in fact the solution with hybridized sp^3 states would have lower energy.

B. sp Solids: Ar, Si and MgO

Having assessed the reliability of our plane-wave pseudopotential implementation of the Perdew-Zunger SIC functional, we now move on to the more interesting case of solids. We choose as our examples face-centered-cubic (FCC) Ar, to make a direct link to the atomic tests reported in the previous subsection, a prototypical semiconductor (Si) and an insulator (MgO); all these materials show the typical LDA underestimation of the band gap. The motivation for investigating these apparently “simple” compounds is to better understand the behavior of the SIC functional in well-known test-case systems, before moving to more complex solids where the description at the LDA level is highly problematic. We use a FCC primitive cell and a simple cubic Born-von Kármán supercell corresponding to a $5 \times 5 \times 5$ ($3 \times 3 \times 3$) k -point meshes in the cases of Si (MgO and Ar). The experimen-

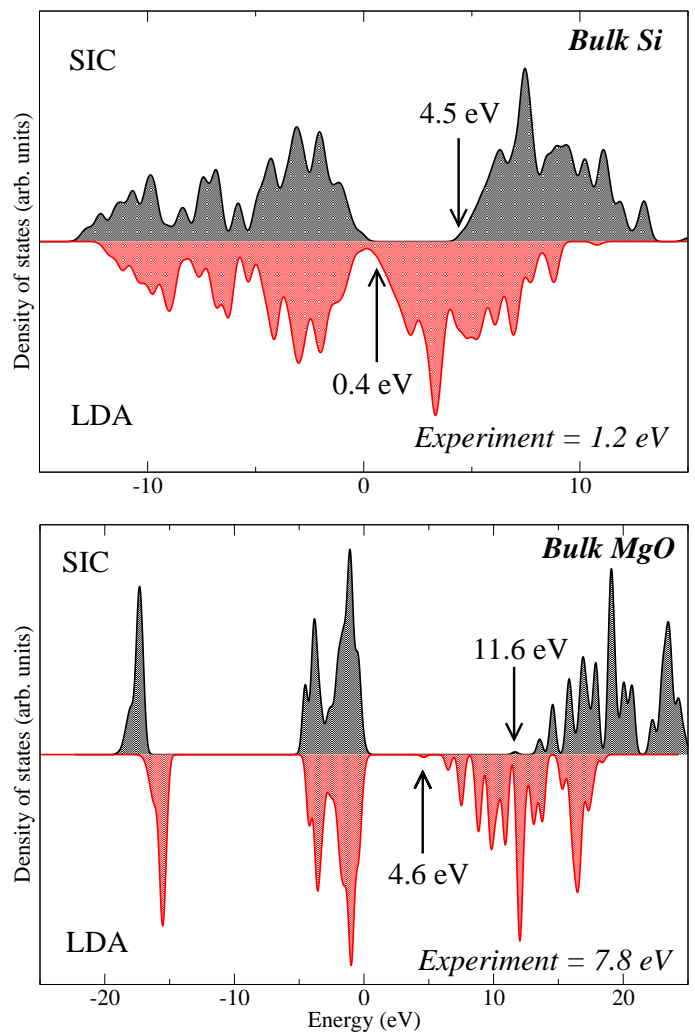


FIG. 1: Density of states for bulk Si (top) and MgO (bottom) calculated within the SIC and LDA approximations. The arrows and numerical values indicate the band gaps in the two approximations to be compared with the experimental values at the bottom right of each plot.

tal lattice constants are used in the Si and MgO cases (10.2 and 7.96 bohr respectively), while the lattice constant is progressively varied in the case of Ar from the experimental value to an artificially compressed state. Plane-wave cut-offs of 50 Ry, 20 Ry, 70 Ry are used in the respective cases of Ar, Si and MgO.

The main goal of the calculations for solid Ar is to quantitatively evaluate the effect of SIC in the transition from the atomic problem to the bulk solid. In particular, we test the statement that “the SIC-LSD approximation provides a mechanism which allows the wave functions to localize for systems where the hopping integrals are small relative to the Coulomb interactions”¹⁰, by tuning the magnitude of the bandwidth, W . We use hydrostatic pressure to vary the bandwidth of the $3p$ band of FCC Ar from the experimental equilibrium volume ($a_0 = 9.9$

a_0 (bohr)	W_{LDA}	E_q^{LDA}	W_{SIC}	E_q^{SIC}	E_{SIC}	Δ_g	$\langle \hat{V}_{SIC} \rangle$
9.9	1.33	8.03	1.38	14.68	-0.45	6.64	-7.05
9.0	2.31	8.54	2.47	15.05	-0.45	6.51	-7.05
8.0	4.38	9.75	4.67	16.25	-0.45	6.50	-7.07
7.0	8.31	12.69	8.84	19.01	-0.44	6.32	-7.12
Atom	-	10.39	-	16.85	-0.46	6.46	-7.07

TABLE I: Bandwidths, W , and band gaps, E_g , calculated within the LDA and SIC approximations for solid Ar over a range of lattice constants. All energies are reported in eV. The last three columns show the SIC energy contribution per electron, E_{SIC} , the SIC correction to the band gap Δ_g and the average of the SIC potential, $\langle \hat{V}_{SIC} \rangle$. The lowest row lists the corresponding values for the isolated atom.

a.u., $W_{LDA}=1.3$ eV) to a highly compressed state ($a_0=7.0$ a.u., $W_{LDA}=8.4$ eV), and monitor the effect of SIC for these extremes together with two intermediate values; the results are reported in Table I.

As expected, the LDA $3p$ bandwidth (W_{LDA}) progressively increases as the crystal is compressed, and the electronic gap increases as well. The same trend is respected in SIC-LDA, with a slightly larger bandwidth (by 0.1-0.5 eV) and a rather dramatic opening of the electronic gap with respect to the corresponding LDA results. The striking fact which is apparent from the Table is that the SIC correction to the electronic gap is practically *independent* of pressure, and amounts exactly to the correction to the $3p$ orbital eigenvalue of the free Ar atom (6.46 eV). Even more striking is the lack of pressure dependence (within numerical error) of both the SIC energy contribution per electron E^{SIC} (-0.44 to -0.46 eV), and the average value of the SIC potential on the corresponding Wannier function (-7.05 to -7.12 eV); this indicates that in this system the SIC is substantially insensitive to the bandwidth of the solid, and corrections are identical to those calculated in the free atom. Most notably, E^{SIC} is almost constant. Therefore, application of the SIC always lowers the variational energy of this system, and there is no crossover to a hypothetical delocalized solution. These results (together with the discussion of atomic Ar in the previous section) strongly suggest that the itinerant character of the oxygen $2p$ bands reported previously¹⁰ is a result of the spherical approximation adopted therein, rather than an intrinsic physical feature of the SIC-LSD method.

Next we move to the cases of Si and MgO. In Fig. 1 we compare the calculated SIC and LDA densities of states and band gaps for both materials at the experimental lattice constants. In all cases the top of the valence band is set to 0 eV. As in the case of solid Ar, the main effect of the SIC is an important stabilization of the valence bands compared to the unoccupied states; otherwise the density of states appears to be almost unaffected, apart from a slight increase of the bandwidth within SIC compared to the LDA ground state. The significant opening of the band-gap leads to a dramatic overcorrection of

the LDA value, especially in the case of bulk Si. The band-gaps within SIC-LDA are respectively 4.5 eV for Si and 11.6 eV for MgO, compared to the LDA (experimental) values of 0.4 (1.2) eV and 4.6 (7.8) eV. This behavior might seem surprising at first sight, especially in silicon where the highly dispersive character of the valence bands leans heavily towards a delocalized (Bloch) description of the electrons rather than a localized one. Our results, however, suggest that even in Si the Wannier functions (which in this case are centered along the Si-Si covalent bonds) are localized enough to carry a significant SIC ($E_{SIC} = -0.24$ eV, $\langle \hat{V}_{SIC} \rangle = -4.58$ eV); this fact further undermines the validity of the SIC-LDA as a theory to discriminate between band insulators and Mott insulators. As a further proof of the localized character of oxygen p bands in solids, we note that our SIC-LDA solution for bulk MgO shows similar behavior to that of the Ar crystal, in that four sp^3 hybrids are formed, each with decidedly negative values of $E_{SIC} = -0.47$ eV and $\langle \hat{V}_{SIC} \rangle = -7.80$ eV.

We are aware of three previous SIC calculations for these materials. HHL⁸ found a correction of 6 eV for the bandgap of solid Ar, which is fairly close to our result in spite of use of the atomic orbital and spherical approximations in the earlier work. FCC Ar was also investigated by Szotek, Temmerman and Winter²⁵, who found an increase of the bandgap of 5.1 eV only, which is in better agreement with our results for the spherically restricted atom. Bulk Si was studied within an approximate bond self-interaction correction by Hatsugai and Fujiwara²⁶, who found a very favorable agreement with the experimental bandstructure, in striking contrast with our results. These data further highlight the fact that the approximations that have been commonly adopted in the literature tend to reduce the systematic, sometimes dramatic, overcorrection of the LDA bandstructure which is obtained within a rigorous application of the SIC-LDA functional.

C. Materials with d electrons

As a first step towards studying the effect of SIC on transition metal compounds we begin with the case of an isolated d -electron atom in a cubic supercell; this allows us to determine the effect of SIC on d states while avoiding complications arising from bandwidth and ligands. In particular, we choose for simplicity the Zn^{2+} ion, which has a completely filled valence shell. Since the Wannier transformation tends to mix wavefunctions that overlap in space, it is necessary to include the semicore $3s$ and $3p$ states explicitly as valence orbitals; the Zn $3s$, $3p$ and $3d$ orbitals have important spatial overlap (see Fig. 3), in spite of being far from each other in energy. As a consequence, the pseudopotentials (Troullier and Martins²⁷, with cutoff radius $r_C=1$ a.u. for all channels) are fairly hard and impose a relatively stiff plane wave cutoff of 180 Ry. We use a cell dimension $a_0 = 16$ a.u. which is

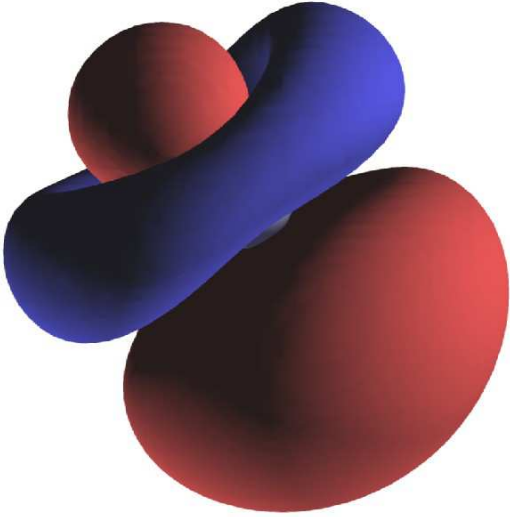


FIG. 2: A representative sp^3d^5 hybrid in the isolated Zn^{2+} ion.

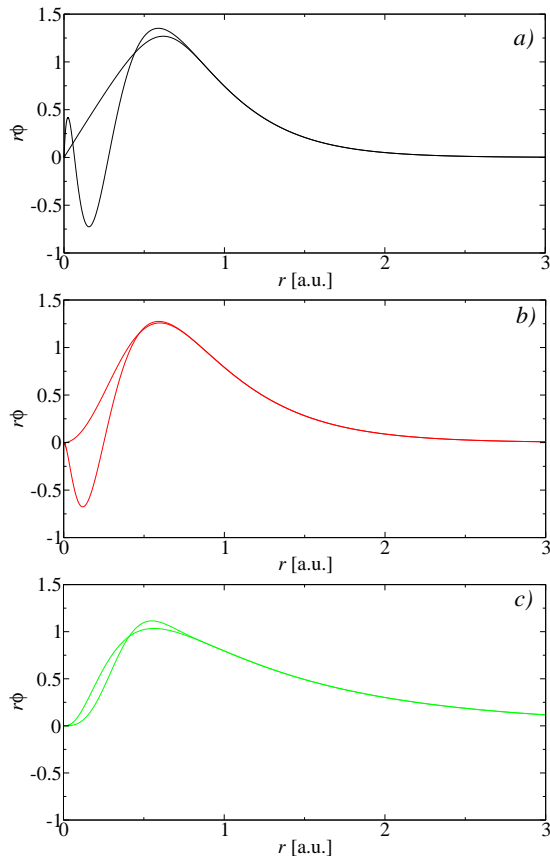


FIG. 3: All-electron and pseudo orbitals for the isolated, neutral Zn atom. a) $3s$; b) $3p$; c) $3d$. Note the large spatial overlap between s , p and d orbitals, whose maximum is located at approximately the same radial distance from the nucleus.

r (bohr)	E_{SIC} (eV)	$\langle \hat{V}_{SIC} \rangle$ (eV)
0.5479	-1.590	-17.972
0.5480	-1.591	-17.976
0.6289	-1.172	-16.548

TABLE II: Radius from the nucleus r , SIC energy contribution per electron, E_{SIC} , and the average of the SIC potential, $\langle \hat{V}_{SIC} \rangle$ calculated for the three groups of sp^3d^5 hybrids in the isolated Zn^{2+} atom.

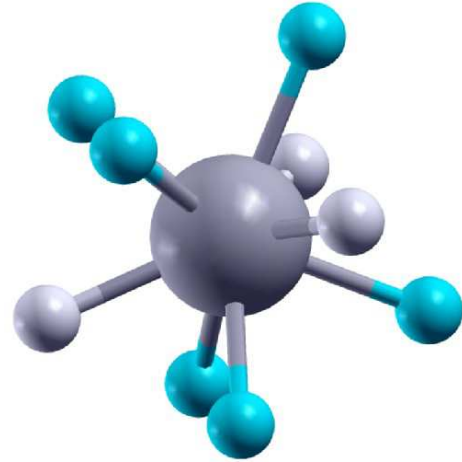


FIG. 4: Position of the centers of the sp^3d^5 orbitals.

large enough so that the spurious crystal-field splitting between e_g and t_{2g} orbitals is small (5×10^{-5} hartree).

Interestingly, the Wannier localization process of Section II yields a set of nine similar-looking sp^3d^5 hybrids (see Fig. 2 for a representative orbital). Upon closer inspection of their Wannier centers and their self-interaction energies, however, these orbitals differ. In fact they are divided into three groups of three members, whose main characteristics are summarized in Tab. II. It is apparent from the Table that the first two groups are practically identical and in fact they form a group of six which is artificially broken into two by the tiny crystal-field splitting imposed by the cubic symmetry of the periodic lattice. The third group, however, is physically distinct. To visualize the splitting we indicate the centers (i.e. the mean value of the position operator) of the orbitals in Fig. 4, by highlighting the members of the group of six as light blue (darker) small spheres and the group of three as white (lighter) small spheres; the position of the Zn ion is indicated by a larger sphere.

Unlike the sp^3 hybrids, which were characterized by tetrahedral symmetry and hence did not cause any splitting in the eigenvalue spectrum within the $3p$ manifold in Ar, the sp^3d^5 hybrids of Zn are therefore inequivalent. This asymmetry is reflected in the eigenvalue spectrum

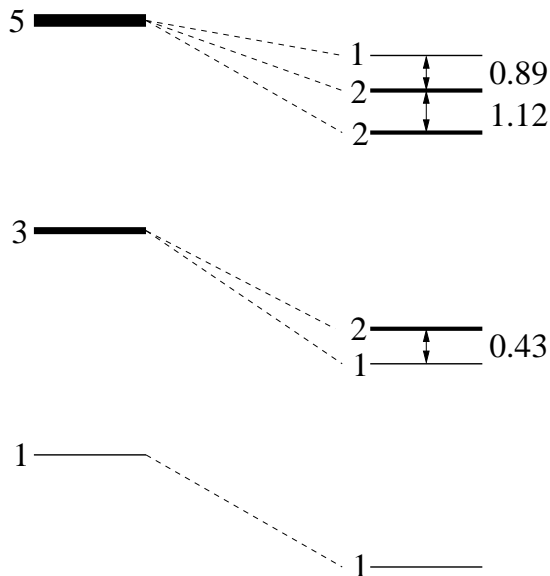


FIG. 5: Schematic diagram of the splittings in the eigenvalue spectrum of the SIC-LDA Hamiltonian for the Zn^{2+} ion. Values are in eV, the spacings are not to scale.

of the SIC-LDA ground state of the Zn^{2+} ion, which is represented in Fig. 5. The $3p$ multiplet, which lies about 100 eV below the vacuum level, is split into a doublet and a singlet by 0.43 eV; however the most dramatic effect is found in the $3d$ electrons, which are extremely important for the complex chemistry of the transition metal compounds. The $3d$ multiplet is split into three levels (2,2,1) by the SIC, with energy separation of 1.12 eV and 0.89 eV, i.e. a total of 2 eV between the lowest and the highest d state. This symmetry breaking and consequent splitting of d levels due to the non-spherical SIC potential was already pointed out by Arai and Fujiwara in Ref. 12. That such a drastically unphysical splitting occurs in a spherically symmetric d electron atom renders the PZ-SIC formalism unreliable for d electron solids, where the interplay of crystal field effects and bandwidth plays a dominant role in determining the overall physical properties of the compound.

IV. DISCUSSION

Our Wannier basis SIC implementation points to two problems in the PZ-SIC formalism. The first, the symmetry breaking and splitting of d levels due to the non-spherical SIC potential is a problem even for the application of PZ-SIC to atoms. The second, the overestimation of the SIE and consequently of splitting in the eigenvalue spectrum and band gaps, becomes more acute in many electron molecules and solids. Concerning the overestimation of the gap, we argue that to correct the LDA bandstructure, not only the local self-interaction of the Wannier charges must be taken into account, but also

(and especially) the *screening* properties of the extended solid upon electron addition/removal; this physical ingredient is completely absent in the PZ-SIC-LDA functional, which is able to capture the dependency on the environment only through the spatial distribution of the Wannier charges. This is insufficient for a complete picture: We have seen in our examples that the effect of the crystal field on the Wannier densities causes remarkably insignificant variations of the SIC correction to the eigenvalue. In particular, for ionic (or rare gas) solids the individual constituents are corrected identically to the isolated ion; this produces a systematic, gross overestimation of band gaps.

The overestimation of the band gap points to two interesting and as yet unanswered questions regarding the physics of the SIE in many-electron systems: What does the self interaction mean in a many-electron system, and how does it relate to electronic relaxation? In particular, a theory that is self-interaction free in the Koopman theorem sense, that is without relaxation corrections, will have over-estimated Hartree-Fock band gaps in the solid. In fact *the self-interaction error is environment-dependent*, and so the relaxation is not distinct from SIE but is intimately related to it. Rigorous theories to incorporate the dependence of the SIE on the dielectric screening environment, such as the GW method, tend to be costly, even if their range of applicability is steadily growing²⁸. Whenever the problem is an ion embedded in a solid with small dispersion and distinct atomic character, atomic approximations can be quite effective. For example, LDA+U has been used recently as an effective technique to cure the SIE, when the value of the Hubbard U parameter is obtained self-consistently within a linear-response approach²⁹ (i.e. it has built-in the dielectric response of the medium); LDA+U is itself close in spirit to the SIC approach, although it was derived from a substantially different starting point. However, when the covalent character of a given compound is stronger (most transition-metal oxides), the reliability of an atomic correction applied only to selected bands becomes questionable, hence the interest for a more uniform treatment of the occupied bands.

A workaround to this problem within SIC-LDA could be to scale down the SIC contribution by a suitable prefactor. This was the approach adopted in the pseudo-SIC formalism of Filippetti and Spaldin¹⁷ where a reduction of the atomic SIC by a factor of 0.5 was included to account for relaxation effects; within full-SIC, Bylaska, Tsemekhman and Gao²² found that a factor of 0.2 was appropriate to describe defects in Si and C compounds. Recent work for molecules³⁰ showed that a scaling factor of $\left(\frac{\tau_\sigma^W}{\tau_\sigma}\right)^k$, where τ_σ is the noninteracting kinetic energy density of σ spin electrons, and $\tau_\sigma^W = \frac{|\nabla\rho_\sigma(r)|^2}{8\rho_\sigma(r)}$ is the Weizsäcker kinetic energy density, gives improved behavior for atoms and molecules. All of these methods improve the agreement with the experimental bandgaps, while still retaining the main physical advantage of SIC:

the Hartree Fock-like treatment of the on-site Coulomb interactions.

Scaling down the SIC, however, does not remove the unphysical symmetry breaking, which is especially serious in d -electron (and presumably f -electron) materials, and is due to the lack of unitary invariance of the functional. Therefore we propose that the most promising route to incorporating the SIC while preserving unitary invariance seems to be the use of hybrid functionals, which incorporate a fraction of HF exchange. Hybrid functionals have yielded very encouraging results for a wide class of systems for the bandgap, structural and electronic properties; the Wannier function methods presented in this work might be useful in devising efficient implementations of the Fock exchange within a plane-wave pseudopotential formalism.

V. CONCLUSIONS

In summary, we have demonstrated that some common problems of SIC-LDA, including multiple local minima and size-consistency issues, can be avoided by lifting the spherical approximation. However, our calculations expose two other serious drawbacks of SIC-LDA. First, we find that the application of the SIC leads to a dramatic overcorrection of the electronic bandgap compared to the LDA solution. Second, we point out a worrisome, unphysical symmetry breaking of spherically symmetric atoms containing d electrons; based on a perturbative analysis we argue that this drawback might be a general feature of state-dependent functionals. Our results highlight the deficiencies of state-dependent corrections to approximate Kohn-Sham theories, and suggest that rotationally invariant corrections (such as the Hartree-Fock exchange in hybrid functionals) are more promising.

APPENDIX A: SYMMETRY BREAKING AND BOYS LOCALIZATION

To better understand whether the origin of this breakdown of spherical symmetry is related to the special features of SIC-LDA or is a more general effect that might concern *any* orbital-dependent functional, it is useful to remove all unnecessary complications and look at the effect of the simplest possible orbital-dependent perturbation on the multiplet structure of a spherically symmetric atom with a filled d shell. A very practical choice is the quadratic spread by Marzari and Vanderbilt, which is better known as Boys quadratic spread in isolated atoms and molecules. Working in the framework of perturbation theory, we start by adding a small contribution to the KS total energy:

$$E^\lambda = E_{KS} + \lambda\Omega, \quad \Omega = \sum_i [(r^2)_i - \bar{r}_i^2] \quad .$$

First we need to minimize Ω with respect to unitary transformations of the occupied orbitals. We start from a representation of angular momentum eigenstates corresponding to the $n = 3$ shell of Zn, i.e. a total of 9 states identified by l and m quantum numbers. It is clear from the above equation that the minimum spread is achieved by maximizing the second terms in the square bracket above (the first is invariant); these are the diagonal elements of the 3D position operator. Equivalently we seek the transformation that *minimizes* the off-diagonal elements of the three projected position operators, which do not commute. The real-space position operators are particularly simple to calculate on this basis, e.g. for \hat{X} we have:

$$\langle lm|\hat{X}|l'm'\rangle = \int \phi_{lm}^*(\mathbf{r})x\phi_{l'm'}(\mathbf{r})d^3r \quad ;$$

x can be written as a real solid harmonic function with $l = 1$:

$$x = -\sqrt{\frac{4\pi}{3}}rY_{1x}(\hat{\mathbf{r}}) \quad ,$$

so that the above matrix element is simply evaluated in terms of a radial integral and a Gaunt coefficient, G :

$$\langle lm|\hat{X}|l'm'\rangle = -\sqrt{\frac{4\pi}{3}} \int_0^\infty r^3 \phi_{lm}^*(r)\phi_{l'm'}(r)dr G_{lm,l'm'}^{1x}.$$

Angular momentum selection rules yield a set of three sparse matrices with zero diagonal elements (angular momentum eigenstates are all centered around the origin) that depend on two values only, which are the sp and pd radial overlaps; the solution to the problem, apart from a trivial scaling factor, is therefore determined by a single parameter. We used the values from the LDA solution of the isolated Zn pseudoatom to construct the three matrices. We then induced a small random unitary mixing to break the symmetry, and we further optimized the quadratic spread to the minimum until we obtained a set of nine sp^3d^5 localized hybrids.

By looking at the positions of the centers (radius from the origin) and at the individual values of the quadratic spread of each hybrid, it is clear that the simplified MV spread functional qualitatively reproduces the same localization pattern which was induced by SIC-LDA. In particular, the orbitals are split into two inequivalent groups, one of six and one of three members; the much smaller splitting of the group of six into two subgroups of three (which was observed in our SIC-LDA atomic calculations) is not reproduced here since in this case we do not use the supercell approach. To appreciate the impact of this perturbation on the Hamiltonian, we now take the functional derivative of Ω with respect to the wavefunctions; since we are at the variational minimum with respect to unitary rotations, this functional derivative yields a well-defined Hermitian operator:

$$\hat{H}^\lambda = \hat{H}_{KS} + \lambda[\hat{R}^2 - 2 \sum_i \bar{r}_i \cdot \langle w_i | \hat{\mathbf{R}}] \quad .$$

The \hat{R}^2 operator is not orbital dependent, but rather a harmonic 3D potential acting on all orbitals which preserves spherical symmetry. The second term in the square bracket, however, does break the symmetry; in particular, it introduces couplings between states belonging to different angular momentum multiplets. The eigenvalues of this operator reproduce qualitatively the splittings observed in the SIC-LDA solution, with the 3 degenerate p states split into 2-1, and the 5 degenerate d

states split into 2-2-1. Therefore, even in the simple case of a harmonic state-dependent perturbation, the spherical symmetry of the isolated atom is broken, and the angular momentum is no longer a good quantum number. This is a very undesirable (and artificial) effect that poses serious problems for the practical applicability of state-dependent potentials to the physics of transition metal oxides.

-
- ¹ M. d’Avezac, M. Calandra, and F. Mauri, Phys. Rev. B **71**, 205210 (2005).
- ² J. VandeVondele and M. Sprik, Phys. Chem. Chem. Phys. **7**, 1363 (2005).
- ³ C. Toher, A. Filippetti, S. Sanvito, and K. Burke, Phys. Rev. Lett. **95**, 146402 (2005).
- ⁴ H. J. Kulik, M. Cococcioni, D. A. Scherlis, and N. Marzari, Phys. Rev. Lett. **97**, 103001 (2006).
- ⁵ A. Ruzsinsky, J. P. Perdew, G. I. Csonka, O. A. Vydrov, and G. E. Scuseria, J. Chem. Phys. **126**, 104102 (2007).
- ⁶ J. P. Perdew, R. G. Parr, M. Levy, and J. L. Balduz, Phys. Rev. Lett. **49**, 1691 (1982).
- ⁷ J. A. Perdew and A. Zunger, Phys. Rev. B **23**, 5048 (1981).
- ⁸ R. A. Heaton, J. G. Harrison, and C. C. Lin, Phys. Rev. B **28**, 5992 (1983).
- ⁹ M. R. Pederson, R. A. Heaton, and C. C. Lin, J. Chem. Phys. **80**, 1972 (1984).
- ¹⁰ A. Svane and O. Gunnarsson, Phys. Rev. Lett. **65**, 1148 (1990).
- ¹¹ Z. Szotek, W. M. Temmerman, and H. Winter, Phys. Rev. B **47**, 4029 (1993).
- ¹² M. Arai and T. Fujiwara, Phys. Rev. B **51**, 1477 (1995).
- ¹³ O. A. Vydrov and G. E. Scuseria, J. Chem. Phys. **122**, 184107 (2005).
- ¹⁴ M. Posternak, A. Baldareschi, S. Massidda, and N. Marzari, Phys. Rev. B **65**, 18442 (2002).
- ¹⁵ N. Marzari and D. Vanderbilt, Phys. Rev. B **56**, 12847 (1997).
- ¹⁶ D. Vogel, P. Krüger, and J. Pollmann, Phys. Rev. B **54**, 5495 (1996).
- ¹⁷ A. Filippetti and N. A. Spaldin, Phys. Rev. B **67**, 125109 (2003).
- ¹⁸ C. D. Pemmaraju, T. Archer, D. Sánchez-Portal, and S. Sanvito, Phys. Rev. B **75**, 045101 (2007).
- ¹⁹ M. Stengel and N. A. Spaldin, PRB **73**, 075121 (2006).
- ²⁰ A. Svane, Phys. Rev. B **53**, 4275 (1996).
- ²¹ S. Goedecker and C. J. Umrigar, Phys. Rev. A **55**, 1765 (1997).
- ²² E. J. Bylaska, K. Tsemekhman, and F. Gao, Physica Scripta **T124**, 86 (2006).
- ²³ G. Makov and M. C. Payne, Phys. Rev. B **51**, 4014 (1995).
- ²⁴ M. Fuchs and M. Scheffler, Comp. Phys. Commun. **119**, 67 (1999).
- ²⁵ Z. Szotek, W. M. Temmerman, and H. Winter, Solid State Comm. **74**, 1031 (1990).
- ²⁶ Y. Hatsugai and T. Fujiwara, Phys. Rev. B **37**, 1280 (1988).
- ²⁷ N. Troullier and J. L. Martins, Phys. Rev. B **43**, 1993 (1991).
- ²⁸ J. B. Neaton, M. S. Hybertsen, and S. G. Louie, Phys. Rev. Lett. **97**, 216405 (2006).
- ²⁹ M. Cococcioni and S. de Gironcoli, Phys. Rev. B **71**, 035105 (2005).
- ³⁰ O. A. Vydrov, G. E. Scuseria, J. P. Perdew, A. Ruzsinszky, and G. I. Csonka, J. Chem. Phys. **124**, 094108 (2006).